Proteins encoded by the *gerP* operon are localised to the inner coat in *Bacillus cereus* spores and are dependent on GerPA and SafA for assembly

Abhinaba Ghosh, James D. Manton, Amin R. Mustafa, Mudit Gupta, Alejandro A. Garcia, Eric J. Rees and Graham Christie*

Department of Chemical Engineering and Biotechnology, University of Cambridge, Cambridge, United Kingdom

*Corresponding author. Phone: +44 1223 334166; Fax: +44 1223 334162

E-mail: gc301@cam.ac.uk

Running title: GerP localisation in spores

Keywords: *Bacillus*, *spore*, *coat*, *germination*, *permeability*

Abstract

Germination of *Bacillus* spores is triggered by certain amino acids and sugar molecules, which permeate through the outermost layers of the spore to interact with receptor complexes that reside in the inner membrane. Previous studies have shown that mutations in the hexacistronic *gerP* locus reduce the rate of spore germination, with experimental evidence indicating that the defect stems from reduced permeability of the spore coat to germinant molecules. Here we use the ellipsoid localisation microscopy technique to reveal that all six *Bacillus cereus* GerP proteins share proximity with cortex lytic enzymes within the inner coat. We reveal also that the GerPA protein alone can localise in the absence of all other GerP proteins, and that it has an essential role for the localisation of all other GerP proteins within the spore. The latter is also demonstrated to be SafA - but not CotE - dependent for localisation, which is consistent with an inner coat location. GerP null spores are shown also to have reduced permeability to fluorescently labelled dextran molecules compared to wild type spores. Overall, the results support the hypothesis that the GerP proteins have a structural role within the spore associated with coat permeability.

Importance

The bacterial spore coat comprises a multi-layered proteinaceous structure that influences the distribution, survival and germination properties of spores in the environment. Results from the current study are significant since they increase our understanding of coat assembly and architecture while adding detail to existing models of germination. We demonstrate also that the ELM image analysis technique can be used as a novel tool to provide direct quantitative measurements of spore coat permeability. Progress in all of these areas should ultimately facilitate improved methods of spore control in a range of industrial, healthcare and environmental sectors.

Introduction

Bacterial endospores (hereafter spores) are ubiquitous in the environment. They are formed by members of the *Bacillales* and *Clostridiales* orders in response to nutrient starvation, the former being aerobic species and the latter anaerobes. Their ubiquity results from the protective cellular structure that the spore represents, as shown in Figure 1. This comprises a central protoplast, or core, which is enveloped, consecutively, by an inner membrane, notable for the reduced fluidity of its lipids, and a thick layer of peptidoglycan, which itself can be subdivided into a structurally distinct germ cell wall and cortex (1). A second membrane – which may be discontinuous - surrounds the cortex, followed by multi-layered coat composed of numerous different proteins. Finally, in some species, the coat itself is surrounded by an outermost structure referred to as the exosporium (2). The various structural features have different primary functions. The coat, for example, protects against degradative enzymes and harmful chemicals (3), whereas the cortex, in conjunction with unique core metabolites such as dipicolinic acid (DPA), results in a protoplast of sufficiently low water activity to ensure metabolic dormancy (4). In this state, bacterial spores can persist in a dormant state in the environment for extended periods of time.

In order to resume the vegetative cell cycle the spore must respond to environmental cues that indicate conditions are once again conducive to growth, all the while being dormant and encased in a multi-layered protective shell. The spore sensing system comprises receptor proteins that are localised to the inner membrane, which respond typically to various amino acids, monosaccharides and inorganic ions (5). Combinations of these germinant molecules are often required to stimulate efficient germinative responses. In spores of *Bacillus* species, presumed binding of germinants to receptor proteins results in the release of Ca^{2+}-DPA and other small molecules from the spore core, followed by the activation of specialised lysins

that degrade the cortical peptidoglycan. These activities permit hydration of the protoplast, resumption of metabolism and – concomitant with shedding of the coat – emergence of a new vegetative cell (5).

A degree of permeability in the spore structure is therefore required to permit the transit of small molecule germinants through the various integument layers to reach and interact with the germinant receptors. In this context, proteins encoded by the hexacistronic *gerP* operon, which is present in the genomes of all *Bacillus* species, have been implicated in having a role in maintaining the permeability of the spore coat. This stems from work conducted initially in *B. cereus* 569, in which spores with a transposon insertion in the operon had a germination defect that could be relieved by chemical removal of the coat (6). Subsequent mutagenesis analyses with *B. subtilis* (7) and *B. anthracis* (8) spores revealed that they too have defective germination phenotypes when the *gerP* operon is disrupted, or in the case of the latter, where individual *gerP* genes are deleted. However, other than being required for efficient spore germination and a suggestion that they are probably coat proteins, little is known of the GerP proteins. Bioinformatic analyses do not reveal any functional clues, only that the various GerP proteins largely resemble orthologous proteins in other species of *Bacillus*. Hence, the purpose of the current study was to use the recently developed ellipsoid localisation microscopy (ELM) technique (9) to more precisely determine the location of the various GerP proteins in *Bacillus cereus* spores. We sought additionally to ascertain whether there is any dependency between the various GerP proteins, and between the GerP and coat morphogenetic proteins, for localisation in the spore. Finally, ELM was used to directly assess the permeability of *gerP* spores to fluorescently labelled dextran molecules compared to wild type spores.

Results

Construction and germination of *B. cereus* 14579 *gerP* strains

Defective spore germination phenotypes associated with the *gerP* operon were first observed in *Bacillus cereus* strain 569 bearing a transposon (Tn917) insertion between *gerPB* and *gerPC* (6). Our initial attempts at creating markerless deletions of the entire *gerP* operon and individual genes within the operon in this strain proved to be unsuccessful. Accordingly, the decision was made to switch the work to *B. cereus* 14579, which appears to be more amenable to genetic manipulation. A markerless allelic exchange system was subsequently used to create a series of strains in the 14579 background where individual genes – start and stop codons aside - from *gerPA* through to *gerPF* were deleted (Tables 1 and S1; Figure S1). The same markerless approach was used to delete the entire *gerP* operon, with the exception of the start codon from *gerPA* and the stop codon of *gerPF* (strain AG007). In common with *B. subtilis* and *B. anthracis*, *B. cereus* 14579 has two additional *gerPF* homologues encoded on the chromosome (BC2276 and BC4794; Table S2), although these were not deleted in the course of this work. Analysis of the resultant null mutant spores by transmission electron microscopy revealed no obvious morphological defects compared to wild type spores (Figure S2).

In order to assess whether deletion of individual or collective *gerP* genes resulted in defective germination phenotypes in the *B. cereus* 14579 background, spores of the various null strains were subjected to a heat shock of 70^{o}C for 15 min, cooled on ice, and their germinative responses to L-alanine and inosine were assessed by monitoring the reduction in absorbance associated with the transition of phase bright dormant spores to phase dark germinated spores. Spores of all strains, apart from the *gerPF* null strain, were defective for germination in buffer supplemented with either alanine or inosine with respect to wild type spores (Figure 2; Figures S3 and S4). The slight reduction in absorbance recorded after 5 min

116 germination of mutant spores appeared to be associated with the germination of a small
117 number of spores within the various populations, at least as adjudged by the light microscope.
118 In contrast, the majority of wild type spores were phase grey or dark after 5 min (data not
119 shown). Even after 60 min, the total loss of absorbance was less than that associated with
120 wild type spores, with microscopy revealing again the presence of many refractile dormant
121 spores in the mutant populations. In all cases, germination defects were restored by
122 complementation with plasmid-borne copies of the deleted gene(s) (Figure S4). In contrast to
123 the above observations, the *gerPF* spore germinative responses to alanine and inosine were
124 indistinguishable from wild type spores, indicating that the homologous genes encoded
125 elsewhere on the chromosome can compensate for the loss of *gerPF*. Additionally, the
126 viability of the various *gerP* null spores was reduced when incubated overnight on rich solid
127 medium, with colony counts for all mutant spores typically 20% of those obtained when
128 plating comparable quantities of wild type spores (data not shown).

129 Spores can also be stimulated to germinate by various non-physiological routes,
130 including by exposure to high concentrations of dipicolinic acid chelated with Ca^{2+} ions
131 (CaDPA) and to the cationic detergent dodecylamine (5). In order to assess the impact of
132 deletion of the various GerP proteins in *B. cereus* 14579 on germination via these routes,
133 spores of the various strains were prepared, incubated in CaDPA or dodecylamine and
134 germination monitored by measuring absorbance loss. In all cases examined germination was
135 reduced compared to that observed with wild type spores, again with the exception of the
136 *gerPF* spores, which showed essentially wild type germinative responses (Figure 2 and
137 Figure S4). Microscopy analyses conducted at the end of each experiment revealed the spore
138 populations to comprise a mixture of predominantly dormant (phase bright) spores
139 interspersed with lower numbers of germinated (phase dark) and partially germinated (phase
140 grey) spores (data not shown). In contrast, wild type spores were essentially all phase dark.

Hence, for both non-nutrient germinative pathways examined, a minority of spores can complete germination whereas most remain dormant.

Localisation of GerP proteins

A series of strains designed to individually express each of the respective GerP proteins as C-terminal GFP fusion proteins was constructed using derivatives of the low copy number pHT315 episomal plasmid. The strategy essentially involved cloning the entire *gerP* operon plus regulatory sequences into pHT315, and then introducing the *gfp* gene in-frame at the 3' end of the gene of interest (minus its stop codon). Individual plasmid constructs – encoding *gerPA-gfp* through to *gerPF-gfp* – were subsequently introduced to wild type cells by electroporation (Table 1), meaning that any expressed fusion proteins would be competing for presumed binding sites within the spore with native GerP proteins expressed from the chromosome. Fluorescence microscopy was used to analyse the various *gfp*-bearing strains cells at intervals throughout sporulation and to examine the final spores in order to observe the pattern of deposition of the various GerP proteins. In all cases expression was observed first as diffuse fluorescence in the mother cell followed by a ring of green fluorescence that developed around the still phase-dark forespore (Figure 3). In some developing spores fluorescence was observed as two hemispheres separated by small junctions at either end of the forespore. Fluorescence was retained in mature spores of all strains (Figure 3), albeit at reduced levels compared to sporulating cells, indicating that the GerP proteins are structural components of the spore rather than being associated purely with the expression or assembly of another component of the spore. Additionally, spores of the various *gfp*-bearing strains appeared to be free of any germination defects in response to both alanine and inosine (Figure S4), indicating in all cases that the GFP moiety was not disruptive to function.

Ellipsoid localisation microscopy was then used to more precisely locate the various GerP proteins in *B. cereus* spores. Information about the location and distribution of proteins in the coat and exosporium of *B. cereus* is sparse in comparison to that available for *B. subtilis* spores. However, previous studies have revealed that the BclA protein forms the fibre-like nap on the exterior surface of the exosporium (10, 11), whereas CotD has been identified as a component of the spore coat (12). Accordingly, strains bearing *gfp*-fusions to the 3' ends of these genes were constructed to serve as benchmarks for the exosporium and coat locations. Strains designed to express C-terminal GFP fusions to SleL and CwlJ were also constructed, since at least in *B. subtilis* these cortex lytic enzymes have been localised to the inner coat (13). Spores of additional strains, including *bxpB-gfp* (BxpB is an exosporium protein (11, 14)), were prepared but failed to show any fluorescence, whereas the irregular distribution of fluorescent foci evident in *cotE-gfp* spores precluded ELM analysis. CotE is important in the assembly of spore outer coat proteins (13), and it may be that the GFP moiety disrupted its key morphogenetic role in our study.

The radial locations of the GerP proteins with respect to the spore centre are shown in Figure 4, together with the numbers of individual spores analysed and the residual fitting error of the ELM measurements. We infer the radial location of GerPA, for example, as 454 nm ± 14 nm in mature spores, where the ± 14 nm is the standard deviation of radial locations found in repeated measurements. GerPB has a radial location of 442 nm (± 23 nm), GerPC 427 nm (± 4 nm), GerPD 407 nm (± 11 nm), GerPE 444 nm (± 10 nm) and GerPF 434 nm (± 10 nm), respectively (Figure 4). As expected, the BclA-GFP protein was measured as having the largest equivalent radius at 566 nm (± 23 nm), which is consistent with its position on the exterior of the spore. Similarly, ELM-derived measurements indicate that the CotD-GFP protein, with an equivalent radius of 484 nm (± 12 nm), is located to the exterior of both SleL-GFP (456 nm, ± 12 nm) and CwlJ-GFP (447, ± 12 nm), with both CLEs apparently

occupying similar locations within the spore. We can infer from these data that the GerP proteins are distributed within the inner spore coat, using the CLEs as indicators of this location. However, the apparent spread of the distribution, coupled with relatively high residuals associated with measurements of some the GerP proteins (stemming from the low brightness of the samples examined) - led us to conduct additional measurements with sporulating cells. Brighter fluorescence and improved separation of cells enabled a greater number of individual cells to be included in the analyses, samples for which were drawn from cultures a few hours prior to release of mature spores from mother cells. In this case, the radial locations of all six GerP proteins was more uniform, averaging 445 nm ± 10 nm. Reduced residual values associated with these measurements increase the level of confidence with which we can state that all six GerP proteins reside in a similar location within the inner spore coat. Additionally, none of the GerP-GFP spores cross-reacted with anti-GFP antisera, which is consistent with an inner-coat location (data not shown).

GerPA dependent localisation

Having established that the various GerP proteins appear to localise to broadly the same vicinity within the spore, we then sought to identify whether the localisation of any individual GerP protein is dependent upon presumed interactions with other protein(s) encoded within the operon. In the first instance this was achieved by introducing variant pHT315 plasmids containing the *gerP* promoter sequence plus an ORF encoding the GerP protein of interest with a C-terminal GFP fusion to strains bearing markerless chromosomal deletions in single *gerP* genes. For example, six plasmids encoding GerPA-GFP through to GerPF-GFP were introduced individually to the *gerPA* background strain (AG001), and then to the *gerPB* background, and so on, creating a total of 36 new strains. Each of these strains was then sporulated by nutrient exhaustion and analysed at intervals by fluorescence microscopy until

mature spores were released. The results of these analyses reveal that in all backgrounds, with the exception of *gerPA*, the various GerP-GFP fusion proteins are expressed and localise around the developing forespore in a manner reminiscent of that observed for GFP fusion proteins in the wild type background (Figure S5). Hence, in the absence of GerPB, for example, all six GFP fusion proteins were observed to localise during sporulation and to persist in the mature spore. The exception to this occurred in the *gerPA* background, where in the absence of GerPA, none of the GerPB – GerPF GFP fusion proteins localised around the developing forespore, although diffuse fluorescence interspersed with bright fluorescent foci was observed in the mother cell in each case (Figure 5). Similar observations were made when the entire *gerP* operon, modified with individual ORFs containing in-frame *gfp* fusions, was expressed in *trans* from a series of plasmids introduced to the *gerP* null background, reducing the potential for differences in expression levels between chromosomal and plasmid borne genes being responsible for the apparent dependency on GerPA for localisation of all other GerP proteins. Similarly, when individual *gerP* genes were introduced on pHT315-derived plasmids to the *gerP* null background only the GerPA-GFP protein was observed to localise and to produce fluorescent mature spores, conferring further evidence that this protein is key to localisation of the other GerP proteins (Figure S6).

GerP dependence on coat morphogenetic proteins

A small number of morphogenetic proteins have been identified from genetic and microscopy-based studies that appear to function as interaction hubs for the recruitment and localisation of defined sub-sets of proteins during the assembly of the *B. subtilis* spore coat (13). The SpoIVA protein, for example, is required for the localisation of proteins that comprise the basement layer of the coat (15), whereas SafA and CotE are responsible, respectively, for localising the inner and outer coat proteins (16, 17). Although details of the

structural hierarchy in terms of morphogenetic protein dependency is sparse in species other than in *B. subtilis*, the conserved presence of genes encoding orthologues of these proteins indicates that SpoIVA, SafA and CotE probably fulfil related functions in most, if not all, *Bacillus* species (1, 13). With this in mind, and with a view to investigating which, if any, of these proteins are crucial to GerP localisation, *spoIVA*, *safA* and *cotE* null mutant strains were prepared in the *B. cereus* 14579 background. Plasmid borne copies of *gerPA-gfp* were introduced subsequently to each mutant strain and sporulation allowed to proceed by nutrient starvation. Microscopy analyses revealed that deletion of *spoIVA* results in early lysis of the developing forespore, hence this strain was not examined any further. In contrast, fluorescence associated with GerPA-GFP was observed in both the *safA* and *cotE* backgrounds (Figure 6). Localisation of the protein, visible as a fluorescent ring encircling the developing forespore, was evident only in the *cotE* background, indicating that GerPA, and presumably by extension all GerP proteins, are SafA dependent proteins.

Measuring the permeability of GerP spores

The seemingly hindered passage of germinant molecules through the spore coats of various species to interact with the inner-membrane located receptors provides an indirect indication of a permeability defect in *gerP* spores. In an attempt to provide a more direct measurement of the permeability of the coats of wild type and mutant spores, we examined the possibility of using ELM to measure the diffusion of FITC-labelled dextrans of differing sizes through the spore coat. Accordingly, both *B. cereus* and *B. subtilis* wild type and *gerP* spores were incubated in solutions of FITC-labelled dextrans ranging in size from 3 kDa to 70 kDa, before examination by fluorescence microscopy as described in the Materials and Methods. The best results in terms of amenability to ELM analysis were obtained with *B. subtilis* spores, for which the fluorescence micrographs showed many well-separated spores with

bright ring-like images indicating that an outer portion of the spore had been fluorescently stained (Figure 7).

Figure 8 presents the mid-point radial locations inferred by ELM analysis for the fluorescent FITC-dextran stains. For every size of FITC-dextran tested, the mid-point of the stained layer was located about 20 nm closer to the spore centre in the wild type spores than in the *gerP* mutants. This is consistent with the notion of impaired coat permeability in the *gerP* mutants that is implied by the germination data; however, the measurement shown in Figure 8, on its own, would also be consistent with the *gerP* mutants simply being larger than the wild type spores, so it is essential to consider this result together with the germination data. Additionally, in both wild type and *gerP* mutants, the smallest dextran molecules (3-5 kDa) were located on average about 15 nm closer to the spore centre than the heavier dextrans. The larger dextrans (10, 20, and 70 kDa) were located in similar regions to one another.

Discussion

Bacterial spores of all species are presented with a dilemma in that their protective structures must prevent ingress of potentially damaging molecules or chemicals to the cellular protoplast within while permitting access of small molecular germinant molecules to the inner-membrane bound germinant receptors. Additionally, they must be capable of rapidly releasing solutes from the spore core, including CaDPA, to the environment upon spore germination. This is achieved, at least in part, by the presence of a multi-layered coat and in some cases exosporium structures, one function of which is to serve collectively as molecular sieves (1). The sieving properties vary between species, but in general it seems that moderately sized proteins and other molecules can breach the outermost layers of spores, exemplified by recent work showing transit of the 26 kDa red fluorescent protein through the

exosporium of *B. megaterium* spores and apparently through the outer – but not inner - coat of *B. subtilis* spores (18, 19). These observations are consistent with earlier studies (20-22), which imply that permeability decreases with progression towards the interior of the spore.

Results of germination experiments conducted in this study with *B. cereus* 14579 spores that are null for the entire *gerP* operon, or individual genes therein, are similarly consistent with previous studies and with the hypothesis that the GerP proteins influence the permeability of the spore coat to small hydrophilic molecules. Defective germinative responses were observed, for example, whether induction was via stimulation of the nutrient germinant receptors by alanine or inosine, or in response to exogenous CaDPA or dodecylamine. The latter is in contrast to results observed in *B. subtilis*, where dodecylamine stimulated a faster germinative response in *gerP* spores compared to wild type spores (7). Dodecylamine is known to trigger germination by stimulating the opening of inner-membrane located DPA channels that are present in both *B. subtilis* and *B. cereus* (5), hence it is not clear why deletion of *gerP* should cause differing germinative responses between species. The exception to the above concerns *B. cereus gerPF* null spores, which displayed essentially wild type germinative responses when stimulated via nutrient or non-nutrient pathways. Presumably the loss of *gerPF* in this case was compensated by either of the two additional *gerPF* homologues encoded elsewhere on the chromosome, as demonstrated previously in closely related *B. anthracis* spores (8).

A primary objective of this study was to ascertain whether the GerP proteins are structural components of the spore or whether they are involved only in spore assembly. Fluorescence microscopy of strains expressing GerP-GFP fusion proteins supports the notion that GerP proteins are indeed located in the spore coat, and the images of smooth fluorescent rings appeared suitable for ELM image analysis using a spherical shell model as an approximation to the GerP-GFP location. We then used ELM to more precisely locate the

315 GerP proteins with respect to some other coat and exosporium proteins. These included the
316 BclA exosporial nap protein, coat-localised CotD, and the CLEs CwlJ and SleL. The radial
317 location of each of these benchmark proteins was established using ELM: BclA, as expected,
318 was outermost, followed by CotD, and then SleL and CwlJ. The SleL and CwlJ proteins
319 occupied a similar radial location around 450 nm, which we identify as the position of the
320 inner coat. Overall, we found that all the GerP proteins were also located in the inner coat.
321 Our analysis of GerP locations in mature spores was, unfortunately, complicated by the fact
322 that the spores tended to clump and hence the number of well-separated spores available for
323 analysis was limited. Additionally, even the available images were often poorly-fitted due to
324 adjacent fluorescent material. The high residual fitting errors shown in Figure 4 indicate that
325 the radial locations found for the GerP proteins in mature spores (407 to 454 nm) have
326 limited accuracy and may be biased by image analysis limitations. In order to obtain more
327 accurate estimates of GerP location, additional fluorescence microscopy was conducted with
328 sporulating GerP-GFP cells in which the fluorescent proteins were observed to have
329 completely localised to rings around phase bright forespores, but prior to mother cell lysis.
330 We obtained superior fluorescence brightness with these samples, and much more
331 importantly we found this removed many of the difficulties due to spore clumping and
332 enabled a higher number of cells to be analysed. Subject to the assumption that the GerP
333 protein locations in these specimens are consistent with their locations in mature spores, we
334 believe this method more accurately located the GerP proteins. These results, in which the
335 GerP protein radial locations span a narrower range from 440 nm to 454 nm, indicate that all
336 six proteins remain in the inner coat, but now seem more likely to share proximity with CwlJ
337 (447 nm) and SleL (456 nm) within the spore (the latter was also observed to occupy a
338 similar location in both sporulating cells and in mature spores). This is an important
339 distinction, since the location of CLEs in the inner spore coat could pose a mechanistic

problem as to how they access the cortical substrate during germination, especially if the GerP proteins form a proteinaceous layer that lies between the CLEs and the cortex/outer membrane boundary. A future objective will be to improve the resolution of these measurements to definitively ascertain the location of CLEs with respect to the cortex.

A further objective of this work was to establish the localisation hierarchy for the GerP proteins, both in terms of morphogenetic protein dependency and to identify any dependency between the individual GerP proteins. With regards to the former, fluorescence microscopy analyses conducted with *B. cereus cotE* and *safA* strains revealed GerPA, and therefore presumably all GerP proteins, to be SafA dependent. Hence, the SafA protein's role as the interaction hub for inner coat localisation in *B. subtilis* spores appears to be conserved in *B. cereus* spores, and again, presumably across all *Bacillus* species. Similar fluorescence microscopy based analyses conducted with a series of null mutants and appropriate GerP-GFP expressing strains indicate that only the GerPA protein is required for each of the remaining GerP proteins to localise in the developing spore. We cannot rule out, however, that one or both of the additional GerPF homologues encoded on the chromosome permit localisation of GerPA-GerPE in the *gerPF* null mutant; this is something that will have to be tested in future. Regardless, we can infer from these analyses that the GerPB, GerPC, GerPD and GerPE proteins each have an essential role in maintaining permeability of the coat to permit ingress of germinants to their sites of interaction with receptors at the inner membrane. GerPA is also essential, although whether this goes beyond its requirement for localisation of the remaining GerP proteins, or whether it has an additional function relating to spore permeability, has yet to be established. Unfortunately, preliminary experiments aimed at identifying physical interactions that may occur between the GerP proteins using a bacterial-2-hybrid system were unsuccessful, owing in part to the relative insolubility of at least some of the proteins when expressed in *E. coli* (data not shown).

Finally, the ELM technique was applied to compare the permeability of wild type and *gerP* spores since it offered the prospect of making direct quantitative measurements using fluorescent dextran stains as opposed to inferring permeability defects based on germination kinetics. Measurements with wild type *B. subtilis* spores revealed that the smallest FITC-dextran tested (3 – 5 kDa) permeated to a depth that is comparable in location to the CotG protein when measured by the same method (radial locations of 473 nm versus 475 nm (9)), whereas the larger dextrans localised to a position comparable to the location of the CotZ outer crust protein (485 nm versus 480 nm (9)). In contrast, mid-point radial locations for all dextran-stained *gerP* spores measured outside the location of the wild type CotZ protein (489 nm for 3 - 5 kDa dextrans and ~505 nm for the larger dextrans). Since CotZ is located on the surface of *B. subtilis* spores (3), these data indicate that none of the dextran stains permeated significantly into the *gerP* spores, adhering and accumulating instead on the spore surface. This may be too simplistic a view, however, since the layer order of proteins in wild type spores may not apply to *gerP* spores, and indeed, a previous study includes a TEM image of a single *B. subtilis gerP* spore that appears to lack the spore crust (23). It is intriguing, therefore, that despite being located in the inner coat, the GerP proteins appear to exert an influence on the permeability of the coat that extends to the surface of the spore. One possible explanation for this is that absence of GerP proteins in the inner coat results in relatively subtle structural perturbations that ripple through to the layers on top, perhaps even leading to loss of the crust. This hypothesis will be tested in future by establishing the layer order and precise locations of defined coat proteins in *gerP* spores with respect to those in wild type spores.

Materials and Methods

Bacterial strains and spore preparation

Bacillus cereus strains employed in this study (Table 1) were all isogenic with the ATCC 14579 strain, which was a gift from Dr. Toril Lindbäck (Norwegian School of Veterinary Science, Norway). *Bacillus cereus* strains were routinely cultured in LB medium at 30^{o}C, supplemented with 1 µg/ml erythromycin and 25 µg/ml lincomycin where appropriate (Table 1). Competent *Escherichia coli* DH5α cells (NEB UK) were used for cloning procedures and for the propagation of plasmids. *Bacillus cereus* spores were prepared by nutrient exhaustion in CCY liquid medium (24). Efficient sporulation was achieved using 200 ml cultures in 2 L baffled flasks that were subject to orbital agitation at 30^{o}C for 48 hours. The resultant spores were purified from cellular debris by centrifuging and resuspending the spore pellets initially in PBS supplemented with 0.1 % (w/v) Tween 20, followed by several rounds of washing and resuspending spores in ice-cold deionised water. Spores of *B. subtilis* strains were prepared by sporulation at 37°C on 2 x Schaeffer's glucose agar plates without antibiotics as described previously (7). Purified spores of both species were stored as suspensions (OD_{600} = 50) in water at 4°C.

Mutant construction

A series of *gerP* null mutant strains in the *B. cereus* 14579 background were constructed using a markerless allelic exchange methodology (19, 25). To delete *gerPA* (BC1145), for example, PCR was used to prepare an amplicon comprising approximately 500 bp of sequence upstream and inclusive of the *gerPA* start codon. A second amplicon comprising 500 bp of downstream sequence starting from, and including the *gerPA* stop codon was also prepared by PCR. Primers were designed to include approximately 15 bp of overlapping sequence between the 3' end of the upstream amplicon and the 5' end of the downstream

amplicon (sequences of primers used in this work are shown in Tables 2 - 5). Additionally, the 5' end of the upstream amplicon contained 15 bp of overlapping sequence with the 5' end of EcoRI and BamHI digested pMAD vector (26), as did the 3' end of the downstream amplicon with the 3' end of pMAD. A variant pMAD vector containing a single I-SceI restriction site was used in this work (a gift from Dr Toril Lindbäck, Norwegian School of Veterinary Science, Oslo). The fragments were assembled using a klenow-based ligation independent cloning technique (https://openwetware.org/wiki/Klenow_Assembly_Method:_Seamless_cloning) and then used to transform *E. coli* to carbenicillin resistance. Transformant *E. coli* were screened by colony PCR to identify clones with the correct construct, and plasmids subsequently purified and validated by DNA sequencing. Similar procedures were used to prepare plasmids designed to individually delete the remaining *gerP* genes (*gerPB* [BC1144], *gerPC* [BC1143], *gerPD* [BC1142], *gerPE* [BC1141], and *gerPF* [BC1140]), and also to delete the entire operon.

pMAD derived plasmids were subsequently introduced to *B. cereus* by electroporation, with transformants being selected at 30^{o}C on LB plates supplemented with 1ug/ml erythromycin, 5ug/ml lincomycin and 90 µg/ml X-gal. Electroporation was conducted using a Gene Pulsar instrument (Biorad), operating at 200 Ω, 2 kV and 25 µF, and cuvettes that contained 500 ng of plasmid DNA plus 50 µl of thawed electrocompetent cells. Clones that had integrated plasmids by homologous recombination were selected by incubating blue colonies at 37^{o}C on fresh LB plates, re-streaking after 24 and 48 hours. Plasmid pBKJ223, which encodes the I-SceI restriction enzyme, was introduced by electroporation to single crossover cells, which were recovered on LB medium containing 10 µg/ml tetracycline. Transformant colonies were subsequently passaged every 24 hours in fresh LB medium containing tetracycline at 37^{o}C, with aliquots being plated and screened on LB agar

438 containing tetracycline and X-gal for white colonies that were sensitive to erythromycin and
439 lincomycin. Candidate colonies that had undergone a second recombination event to excise
440 the integrated plasmid, leaving behind the truncated gene, were validated by PCR and
441 sequencing, and then passaged on LB medium minus antibiotics to promote excision of the
442 pBKJ223 plasmid. The same markerless deletion strategy was used to create *B. cereus* 14579
443 derived strains that were null for the coat morphogenetic proteins SpoIVA (BC1509), SafA
444 (BC4420), and CotE (BC3770).

445 The low copy number episomal plasmid pHT315 (27) was used as the basis to
446 construct a series of GerP-GFP fusion strains. Two different strategies were employed. First,
447 overlap PCR was used to construct six variant *gerP* operons, each of which contained the
448 native promoter sequence followed by *gerPA* through to *gerPF*. In each variant plasmid a
449 single *gerP* gene, minus stop codon, was fused at the 3'end with an amplicon encoding the
450 gene for GFP. Fragments containing the *gerP* promoter sequence, variant *gerP* operons, and
451 linearised pHT315 were assembled using the klenow assembly technique, and used to
452 transform *E. coli* to carbenicillin resistance. A similar approach was used to construct
453 pHT315-derived plasmids containing the *gerP* promoter sequence and single *gerP* genes
454 fused at the 3'end with *gfp*. Constructs containing *gfp* fusions to *bclA* (BC1207), *cotD*
455 (BC1560), *sleL* (BC3607) and *cwlJ* (BC5390), each under control of their native promoter
456 sequences, were prepared similarly. In all cases, the resultant plasmids were purified from
457 positive *E. coli* clones, validated for the intended construction by DNA sequencing, and
458 introduced to *B. cereus* wild type and *gerP* null strains by electroporation.

459

460 **Spore germination assays**

461 Spore germination assays were conducted using spores that were synchronised to germinate
462 by incubating at 70^{o}C for 15 min and then cooled on ice. Spores (300 µl) were resuspended

463 at an optical density at 600 nm (OD_{600}) of 1 (approx. 10^8 spores ml^{-1}) in 10 mM Tris-HCl
464 buffer, pH 7.4, supplemented with 10 – 100 mM L-alanine or inosine and the resultant
465 changes in absorbance were monitored at 30°C using a Perkin-Elmer EnVision-Xcite
466 multilabel plate reader fitted with a 600-nm photometric filter. Germination experiments
467 conducted with non-physiological germinants were conducted by resuspending spores at an
468 OD_{600} of 1 in 2.5 mM Tris-HCl, pH 7.4, supplemented with 50 mM CaDPA at 30°C, or in 25
469 mM KPO_4, pH 7.5, supplemented with 1 mM dodecylamine at 45°C. Changes in absorbance
470 of the spore suspensions were monitored as above. Presented data are from single
471 experiments, which are representative of multiple analyses conducted with at least two
472 batches of spores. Spore viability was assessed by plating serially diluted spore suspensions
473 on LB agar plates, followed by colony enumeration after 24 hours incubation at 30°C.
474
475 **Microscopy**
476 Three µL of spore or cellular suspensions were dispersed onto poly-L-lysine coated
477 microscope slides, and sealed under a coverslip. The samples were imaged on an Olympus
478 BX53 microscope with a 100X 1.30 NA oil objective lens, illumination from a mercury lamp
479 and filters for GFP and red fluorescence (i.e. FM4-64 dye was added to some samples to
480 enable visualisation of membranes). Images were captured with a Retiga-2000R CCD
481 camera, giving a pixel width of 74 nm on the specimen, and 12 bit grey levels. Image data
482 was recorded as 1600x1200 pixel Tiffs.
483
484 **Immunolabelling of spores**
485 Spores (1 ml, OD_{600} = 10) were incubated with gentle agitation at room temperature in
486 phosphate-buffered saline (PBS) containing 2% (w/v) bovine serum albumin (BSA) for 1 h.
487 Spores were harvested by centrifugation (13,500 x g for 1 min), resuspended in 400 µl PBS–

BSA and incubated with 100 µl of 500-fold diluted anti-GFP antibody (ab290; Abcam, Cambridge, UK) for 30 min, followed by three washes in PBS–BSA. Resuspended spores (400 µl) were then incubated with 100 µl of 500-fold diluted Dylight594-conjugated anti-rabbit IgG antibody (ab96885; Abcam), for 30 min. Antibody labelled spores were washed three times with PBS–BSA and then analysed by fluorescence microscopy.

Dextran permeability experiments

A series of fluorescein isothiocyanate (FITC) labelled dextrans (Sigma-Aldrich, Dorset, UK), with average molecular masses of 3 – 5 kDa, 10 kDa, 20 kDa and 70 kDa, were used to investigate the permeability of *B. subtilis* wild type and *gerP* spores. Essentially, 50 µl of the respective FITC-dextran solutions (25 mg/ml) were added to the same volume of spores (OD_{600} = 10), which were then incubated for 24 h at 4^{o}C. In order to reduce background fluorescence, the dextran-spore suspensions were pelleted by centrifugation (13,500 x *g* for 1 min), enabling removal of the unbound dextran-containing supernatant, before resuspending the spores in 1 ml of sterile DI water. The spores were centrifuged again, resuspended in 100 µl of water, and then 3 µl of the suspension transferred to poly-L-lysine coated microscope slides for imaging by fluorescence microscopy.

Ellipsoid localisation microscopy

The quantitative fluorescence ELM technique was used to measure the location of GFP fusion proteins in mature spores and in sporulating cells, and also to measure the extent to which fluorescently labelled dextran molecules had permeated into spores. The ELM analysis has previously been reported in detail (9). Briefly, several independent fields of GFP or FITC-dextran labelled spores or sporulating cells were imaged with fluorescence microscopy. Each field contained about 50 spores or cells on a dark background. Automated image

segmentation was used to identify single spores, and the image of each candidate was used to fit the parameters of a model that describes the image of a spheroidal fluorescent shell. For *B. cereus*, an equation describing the image of a spherical fluorescent layer was fitted to the image data; for *B. subtilis* a model for an ellipsoidal shell was fitted because this spore cannot be well-approximated by a sphere. A filter was applied to exclude fits from overlapping spores and fragments of debris. The average radius parameter fitted to the spores provides an estimate of the mid point radial position of the GFP fusion or FITC-dextran layer with respect to the spore centre. (The equivalent radius of a sphere of equal volume is reported for FITC-dextran layers that were analysed with the ellipsoid model.) The mean and standard deviation of the estimates from several fields of spores or cells with each protein are presented in Figures 4 and 8. Sample data and ELM software are provided in supporting data (https://doi.org/10.17863/CAM.13158).

Acknowledgements

The authors declare no competing financial interests. AG was the recipient of a Cambridge Nehru Scholarship and received support from the Raymond and Beverly Sackler Foundation. We gratefully acknowledge support from MedImmune through the Beacon collaboration, and from the Engineering and Physical Sciences Research Council Centre for Doctoral Training in Sensor Technologies and Applications (EP/L015889/1).

References

1. Henriques AO, Moran CP. 2007. Structure, Assembly, and Function of the Spore Surface Layers. Annual Review of Microbiology 61:555-588.

2. Stewart GC. 2015. The Exosporium Layer of Bacterial Spores: a Connection to the Environment and the Infected Host. Microbiol Mol Biol Rev 79:437-457.

3. McKenney PT, Driks A, Eichenberger P. 2013. The *Bacillus subtilis* endospore: assembly and functions of the multilayered coat. Nature reviews Microbiology 11:33-44.

4. Popham DL, Bernhards CB. 2015. Spore Peptidoglycan. Microbiol Spectr 3.

5. Setlow P. 2014. Germination of Spores of *Bacillus* Species: What We Know and Do Not Know. J Bacteriol 196:1297-1305.

6. Behravan J, Chirakkal H, Masson A, Moir A. 2000. Mutations in the *gerP* locus of *Bacillus subtilis* and *Bacillus cereus* affect access of germinants to their targets in spores. J Bacteriol 182:1987-1994.

7. Butzin XY, Troiano AJ, Coleman WH, Griffiths KK, Doona CJ, Feeherry FE, Wang G, Li YQ, Setlow P. 2012. Analysis of the effects of a *gerP* mutation on the germination of spores of *Bacillus subtilis*. J Bacteriol 194:5749-5758.

8. Carr KA, Janes BK, Hanna PC. 2010. Role of the *gerP* operon in germination and outgrowth of *Bacillus anthracis* spores. PLoS One 5:e9128.

9. Manetsberger J, Manton JD, Erdelyi MJ, Lin H, Rees D, Christie G, Rees EJ. 2015. Ellipsoid Localization Microscopy Infers the Size and Order of Protein Layers in *Bacillus* Spore Coats. Biophys J 109:2058-2066.

10. Sylvestre P, Couture-Tosi E, Mock M. 2002. A collagen-like surface glycoprotein is a structural component of the *Bacillus anthracis* exosporium. Mol Microbiol 45:169-178.

11. Todd S, Moir A, Johnson M, Moir A. 2003. Genes of *Bacillus cereus* and *Bacillus anthracis* Encoding Proteins of the Exosporium. J Bacteriol 185:3373-3378.

12. Eijlander RT, Kuipers OP. 2013. Live-cell imaging tool optimization to study gene expression levels and dynamics in single cells of *Bacillus cereus*. Appl Environ Microbiol 79:5643-5651.

13. Driks A, Eichenberger P. 2016. The Spore Coat. Microbiol Spectr 4.

14. Steichen CT, Kearney JF, Turnbough CL, Jr. 2005. Characterization of the exosporium basal layer protein BxpB of *Bacillus anthracis*. J Bacteriol 187:5868-5876.

15. Ramamurthi KS, Losick R. 2008. ATP-driven self-assembly of a morphogenetic protein in *Bacillus subtilis*. Mol Cell 31:406-414.

16. Little S, Driks A. 2001. Functional analysis of the *Bacillus subtilis* morphogenetic spore coat protein CotE. Mol Microbiol 42:1107-1120.

17. Ozin AJ, Henriques AO, Yi H, Moran CP, Jr. 2000. Morphogenetic proteins SpoVID and SafA form a complex during assembly of the *Bacillus subtilis* spore coat. J Bacteriol 182:1828-1833.

18. Donadio G, Lanzilli M, Sirec T, Ricca E, Isticato R. 2016. Localization of a red fluorescence protein adsorbed on wild type and mutant spores of *Bacillus subtilis*. Microb Cell Fact 15:153.

19. Lindback T, Mols M, Basset C, Granum PE, Kuipers OP, Kovacs AT. 2012. CodY, a pleiotropic regulator, influences multicellular behaviour and efficient production of virulence factors in *Bacillus cereus*. Environ Microbiol 14:2233-2246.

20. Gerhardt P, Black SH. 1961. Permeability of bacterial spores. II. Molecular variables affecting solute permeation. J Bacteriol 82:750-760.

21. Koshikawa T, Beaman TC, Pankratz HS, Nakashio S, Corner TR, Gerhardt P. 1984. Resistance, Germination, and Permeability Correlates of *Bacillus megaterium* Spores Successively Divested of Integument Layers. J Bacteriol 159:624-632.

22. Nishihara T, Takubo Y, Kawamata E, Koshikawa T, Ogaki J, Kondo M. 1989. Role of Outer Coat in Resistance of *Bacillus megaterium* Spore. J Biochem 106:270-273.

23. Nagler K, Setlow P, Reineke K, Driks A, Moeller R. 2015. Involvement of Coat Proteins in *Bacillus subtilis* Spore Germination in High-Salinity Environments. Appl Environ Microbiol 81:6725-6735.

24. Xu Zhou K, Wisnivesky F, Wilson DI, Christie G. 2017. Effects of culture conditions on the size, morphology and wet density of spores of *Bacillus cereus* 569 and *Bacillus megaterium* QM B1551. Lett Appl Microbiol 65:50-56.

25. Janes BK, Stibitz S. 2006. Routine markerless gene replacement in *Bacillus anthracis*. Infect Immun 74:1949-1953.

26. Arnaud M, Chastanet A, Debarbouille M. 2004. New vector for efficient allelic replacement in naturally nontransformable, low-GC-content, gram-positive bacteria. Appl Environ Microbiol 70:6887-6891.

27. Arantes O, Lereclus D. 1991. Construction of cloning vectors for *Bacillus thuringiensis*. Gene 108:115-119.

603 Table 1 *Bacillus* strains used in this study

604

Strain	Relevant phenotype or genotype [a]	Source or reference
***B. subtilis* strains**		
PS832	Wild type	Peter Setlow
PS4228	Δ*gerP* Tc^r	Peter Setlow
***B. cereus* strains**		
14579	Wild type	Toril Lindbäck
AG001	Δ*gerPA*	This study
AG002	Δ*gerPB*	This study
AG003	Δ*gerPC*	This study
AG004	Δ*gerPD*	This study
AG005	Δ*gerPE*	This Study
AG006	Δ*gerPF*	This study
AG007	Δ*gerP*	This study
AM001	Δ*spoIVA*	This study
AM002	Δ*safA*	This study
AM003	Δ*cotE*	This study
Mutant transformants		
AG008	Δ*gerPA*::pHT315-Promoter-*gerPA* MLS^r	This study
AG009	Δ*gerPB*::pHT315-Promoter-*gerPB* MLS^r	This study
AG010	Δ*gerPC*::pHT315-Promoter-*gerPC* MLS^r	This study
AG011	Δ*gerPD*::pHT315-Promoter-*gerPD* MLS^r	This study
AG012	Δ*gerPE*::pHT315-Promoter-*gerPE* MLS^r	This study
AG013	Δ*gerPF*::pHT315-Promoter-*gerPF* MLS^r	This study
AG014	Δ*gerP*::pHT315-Promoter-*gerP* MLS^r	This study
GerP localisation strains		
AG015	pHT315-Promoter-*PA-gfp-PB-PC-PD-PE-PF* MLS^r	This study
AG016	pHT315-Promoter-*PA-PB-gfp-PC-PD-PE-PF* MLS^r	This study

AG017	pHT315-Promoter-*PA-PB-PC-gfp-PD-PE-PF* MLS^r	This study
AG018	pHT315-Promoter-*PA-PB-PC-PD-gfp-PE-PF* MLS^r	This study
AG019	pHT315-Promoter-*PA- PB-PC-PD-PE-gfp-PF* MLS^r	This study
AG020	pHT315-Promoter-*PA-PB-PC-PD-PE–PF-gfp* MLS^r	This study
Dependency studies		
AM004	Δ*spoIVA*::pHT315-Promoter-*gerPA-gfp* MLS^r	This study
AM005	Δ*safA*::pHT315-Promoter-*gerPA-gfp* MLS^r	This study
AM006	Δ*cotE*::pHT315-Promoter-*gerPA* MLS^r	This study
AG022	Δ*gerPA*::pHT315-Promoter-*gerPA-gfp* MLS^r	This study
AG023	Δ*gerPA*::pHT315-Promoter-*gerPB-gfp* MLS^r	This study
AG024	Δ*gerPA*::pHT315-Promoter-*gerPC-gfp* MLS^r	This study
AG025	Δ*gerPA*::pHT315-Promoter-*gerPD-gfp* MLS^r	This study
AG026	Δ*gerPA*::pHT315-Promoter-*gerPE-gfp* MLS^r	This study
AG027	Δ*gerPA*::pHT315-Promoter-*gerPF-gfp* MLS^r	This study
AG028	Δ*gerPB*::pHT315-Promoter-*gerPA-gfp* MLS^r	This study
AG029	Δ*gerPB*::pHT315-Promoter-*gerPB-gfp* MLS^r	This study
AG030	Δ*gerPB*::pHT315-Promoter-*gerPC-gfp* MLS^r	This study
AG031	Δ*gerPB*::pHT315-Promoter-*gerPD-gfp* MLS^r	This study
AG032	Δ*gerPB*::pHT315-Promoter-*gerPE-gfp* MLS^r	This study
AG033	Δ*gerPB*::pHT315-Promoter-*gerPF-gfp* MLS^r	This study
AG034	Δ*gerPC*::pHT315-Promoter-*gerPA-gfp* MLS^r	This study
AG035	Δ*gerPC*::pHT315-Promoter-*gerPB-gfp* MLS^r	This study
AG036	Δ*gerPC*::pHT315-Promoter-*gerPC-gfp* MLS^r	This study
AG037	Δ*gerPC*::pHT315-Promoter-*gerPD-gfp* MLS^r	This study
AG038	Δ*gerPC*::pHT315-Promoter-*gerPE-gfp* MLS^r	This study
AG039	Δ*gerPC*::pHT315-Promoter-*gerPF-gfp* MLS^r	This study
AG040	Δ*gerPD*::pHT315-Promoter-*gerPA-gfp* MLS^r	This study
AG041	Δ*gerPD*::pHT315-Promoter-*gerPB-gfp* MLS^r	This study

AG042	Δ*gerPD*::pHT315-Promoter-*gerPC-gfp* MLS^r	This study
AG043	Δ*gerPD*::pHT315-Promoter-*gerPD-gfp* MLS^r	This study
AG044	Δ*gerPD*::pHT315-Promoter-*gerPE-gfp* MLS^r	This study
AG045	Δ*gerPD*::pHT315-Promoter-*gerPF-gfp* MLS^r	This study
AG046	Δ*gerPE*::pHT315-Promoter-*gerPA-gfp* MLS^r	This study
AG047	Δ*gerPE*::pHT315-Promoter-*gerPB-gfp* MLS^r	This study
AG048	Δ*gerPE*::pHT315-Promoter-*gerPC-gfp* MLS^r	This study
AG049	Δ*gerPE*::pHT315-Promoter-*gerPD-gfp* MLS^r	This study
AG050	Δ*gerPE*::pHT315-Promoter-*gerPE-gfp* MLS^r	This study
AG051	Δ*gerPE*::pHT315-Promoter-*gerPF-gfp* MLS^r	This study
AG052	Δ*gerPF*::pHT315-Promoter-*gerPA-gfp* MLS^r	This study
AG053	Δ*gerPF*::pHT315-Promoter-*gerPB-gfp* MLS^r	This study
AG054	Δ*gerPF*::pHT315-Promoter-*gerPC-gfp* MLS^r	This study
AG055	Δ*gerPF*::pHT315-Promoter-*gerPD-gfp* MLS^r	This study
AG056	Δ*gerPF*::pHT315-Promoter-*gerPE-gfp* MLS^r	This study
AG057	Δ*gerPF*::pHT315-Promoter-*gerPF-gfp* MLS^r	This study
AG058	Δ*gerP*::pHT315-Promoter-*gerPA-gfp* MLS^r	This study
AG059	Δ*gerP*::pHT315-Promoter-*gerPB-gfp* MLS^r	This study
AG060	Δ*gerP*::pHT315-Promoter-*gerPC-gfp* MLS^r	This study
AG061	Δ*gerP*::pHT315-Promoter-*gerPD-gfp* MLS^r	This study
AG062	Δ*gerP*::pHT315-Promoter-*gerPE-gfp* MLS^r	This study
AG063	Δ*gerP*::pHT315-Promoter-*gerPF-gfp* MLS^r	This study

MLS^r, macrolide-lincosamide-streptogramin-B resistance

608 Table 2 Oligonucleotide primers used to create null mutant strains

Strain	Primer	Sequence (5' to 3')
gerPA	pMAD *gerPA* up For	CCATGGTACCCGGGAGCTCGAATTCCT CATACCCTTTAATTGTATTCGCA
	ATGTAA *gerPA* up Rev	AAAAATTCAATGCAATTGCCTCCTTTAC ATACAAAACACCCTTCGTTTTT
	ATGTAA *gerPA* down For	AAAAACGAAGGGTGTTTTGTATGTAAA GGAGGCAATTGCATTGAATTTTT
	pMAD *gerPA* down Rev	GCCTCGCGTCGGGCGATATCGGATCCA AACCAATATTTAAAGTACCATTT
gerPB	pMAD *gerPB* up For	GCCATGGTACCCGGGAGCTCGAATTCG CGATTGAAAAAAAACGTGAAAAA
	ATGTAA *gerPB* up Rev	ATATTTATGACAAGGATGTCTTACATTG CAATTGCCTCCTTTAAGTTGAG
	ATGTAA *gerPB* down For	GCTCAACTTAAAGGAGGCAATTGCAAT GTAAGACATCCTTGTCATAAATA
	pMAD *gerPB* down Rev	GCCTCGCGTCGGGCGATATCGGATCCC ATCCACCATCATTTGTCGATACA
gerPC	pMAD *gerPC* up For	GCATGCCATGGTACCCGGGAGCTCGAA TTCTGGTCGGACATATTCGTATC
	ATGTAA *gerPC* up Rev	CGTTAAGGTTCATACATACTTACATTTG TGAAACCTCCTTTTCAATAGGG
	ATGTAA *gerPC* down For	CCCTATTGAAAAGGAGGTTTCACAAAT GTAAGTATGTATGAACCTTAACG
	pMAD *gerPC* down Rev	GCCTCGCGTCGGGCGATATCGGATCCA AAAGTGTGCGCAATTCAACGTTA
gerPD	pMAD *gerPD* up For	GCATGCCATGGTACCCGGGAGCTCGAA TTCAAAATCGCCCCTCCTCTTCT
	ATGTAA *gerPD* up Rev	ATAATTTTTCAGTCTCCTTACATACATA CTTACTCCTTTCGGAAATTTC
	ATGTAA *gerPD* down For	GAAATTTCCGAAAGGAGTAAGTATGTA TGTAAGGAGACTGAAAAATTAT
	pMAD *gerPD* down Rev	CCTCGCGTCGGGCGATATCGGATCCAA TTGAAAGAACCGTTACTGTTTTG
gerPE	pMAD *gerPE* up For	TGCATGCCATGGTACCCGGGAGCTCGA ATTCAAAATCGCCCCTCCTCTTC
	ATGTAA *gerPE* up Rev	CATAATTTTTCAGTCTCCTTACATACAT ACTTACTCCTTTCGGAAATTTC
	ATGTAA *gerPE* down For	GAAATTTCCGAAAGGAGTAAGTATGTA TGTAAGGAGACTGAAAAATTATG
	pMAD *gerPE* down Rev	GCCTCGCGTCGGGCGATATCGGATCCA ATTGAAAGAACCGTTACTGTTTTG
gerPF	pMAD *gerPF* up For	TGCATGCCATGGTACCCGGGAGCTCGA ATTCAACAGTTACAGAGGGTCCA
	ATGTAA *gerPF* up Rev	AGAATATCTCCTACTTTTTTTACATCCA CCTACTTTACTAAACTTTGTAA
	ATGTAA *gerPF* down For	TTACAAAGTTTAGTAAAGTAGGTGGAT GTAAAAAAAGTAGGAGATATTCT

	pMAD *gerPF* down Rev	CCTCGCGTCGGGCGATATCGGATCCAA CATCCTGTAAAAGAGAAATGTTT
gerP (operon)	pMAD *gerP* up For	GCCATGGTACCCGGGAGCTCGAATTCT CTCCATCCTAAAACT
	ATGTAA *gerP* up Rev	CTTGTTTATACCACTATTACATTTATTG CGTGTGTGTTTTGAACG
	ATGTAA *gerP* down For	CGTTCAAAACACACACGCAATAAATGT AATAGTGGTATAAACAAGTAAG
	pMAD *gerP* down Rev	GCCTCGCGTCGGGCGATATCGGATCCA GAAAAGCTTACAACATCCTGT
cotE	pMAD *cotE* up For	CCATGGTACCCGGGAGCTCGAATTCAT TTCTGAAACAGAAGAAGTTGATT
	ATGTAA *cotE* up Rev	ACTTCTCCCTAGCTTTCTATTACATTCG TAACCCTCCTCAATCACTATTC
	ATGTAA *cotE* down For	TAGAAAGCTAGGGAGAAGTTCTTCC
	pMAD *cotE* down Rev	CCTCGCGTCGGGCGATATCGGATCCAA TTGTACTACTTCACGACGTACTA
safA	pMAD *safA* up For	CCATGGTACCCGGGAGCTCGAATTCAT ATGATTGAATCAGCGCCACCTGG
	ATGTAA *safA* up Rev	CGGGAATACTCCCGCCTTTTTACATATT TTCCCCCTCCTGTATAACTTAT
	ATGTAA *safA* down For	AAATATGTAAAAAGGCGGGAGTATTCC CGCCTTTT
	pMAD *safA* down Rev	CCTCGCGTCGGGCGATATCGGATCCCT GTTTTACCATCATTGTTAATGTA

609

610 Table 3 Oligonucleotide primers used to validate null mutant strains by diagnostic PCR

Strain	Primer	Sequence (5’ to 3’)
gerPA	*gerPA* Out For	GTCATGTACATACGGATTTACACCCTAATC AAACGTTCAAAACACACACG
	gerPA Out Rev	GATAGGGCTTTAATACTTCCGGCAGTACC AATTTGGAACACAGAAGAGG
gerPB	*gerPB* Out For	CCGGCTCTTTCAACGTTGGAGATAATGTTT CTGTCTACAATTATCA
	gerPB Out Rev	GCTCTTCTTGGAGTTGGCGCACTTGATCTT CTAAATTTAGGATGGCTGC
gerPC	*gerPC* Out For	GGTACTGCCGGAAGTATTAAAGCCCTATC TAAATTTTCAAATACGGGCGG
	gerPC Out Rev	CGGACGACGATACACCGTTCATTTTAATCT GTCCGACTTTTAACTCACGG
gerPD	*gerPD* Out For	GCATCGACTCCCTTATTATTTATCACAAGC GCAATCATATGAAGGTA
	gerPD Out Rev	CTCCCCGTATATAACAAGGAATTTCACGG TGGACGGCAATAGCTCTAC

gerPE	*gerPE* Out For	GCCTTTCTCTCCTTTATTCAGCACATACCG GGAAATTTCCGAAAGGAG
	gerPE Out Rev	GATCTGCCACATCAGAATCAAATGTATTC GTTGCACTAACACCGTTAAAC
gerPF	*gerPF* Out For	GCGCACACTTTTAAACTCTGGTGGATTTCA AATTGGAAATGTTGATTATG
	gerPF Out Rev	TAGTGCCTCTTCACTACTTACTTGTTTATA CCACTATTTGTGGAC
gerP	*gerP* Out For	CGGCGCTAATATTTTCACCTCTGTTAACGG ATAATACGCCGCTTCCCCG
	gerP Out Rev	GATGCTTGCAGCAGAAGAAGCATATCAAG ATTGGCAAGGGAAGAGTG

611

612 Table 4 Oligonucleotide primers used to create GFP fusion strains

Primer	Sequence (5' to 3')	Overlap
gfp For	AGTAAAGGAGAAGAACTTTTCACTGGAGTTG TCCCAATTCTTGTTGAATT	
gfp Rev	TTATTTGTATAGTTCATCCATGCCATGTGTAA TCCCAGCAGCTGTTACAA	
pHT315 Prom *gerPA* For	CAGCTATGACCATGATTACGCCAAGCTTTCAT TTGGCATAAAATGTAG	pHT315
pHT315 *gerPF* Rev	GTTGTAAAACGACGGCCAGTGAATTCTTACG CTGTTCCAATCTGATCTTG	pHT315
gfp gerPA Rev	CCAGTGAAAAGTTCTTCTCCTTTACTAGTTGA GCCAATTATCGCTTGATC	*gfp*
gfp gerPB For	GCATGGATGAACTATACAAATAAAGGAGGCA ATTGCATTGAATTTTTA	*gfp*
gfp gerPB Rev	GTGAAAAGTTCTTCTCCTTTACTAGAAGAACT AGTTGATGGTTTGATAG	*gfp*
gfp gerPC For	GGCATGGATGAACTATACAAATAAGACATCC TTGTCATAAATATATAGCA	*gfp*
gfp gerPC Rev	CCAGTGAAAAGTTCTTCTCCTTTACTCTCCTTT CGGAAATTTCCCGGTAT	*gfp*
gfp gerPD For	GGCATGGATGAACTATACAAATAAGTATGTA TGAACCTTAACGTTGTAAA	*gfp*
gfp gerPD Rev	CTCCAGTGAAAAGTTCTTCTCCTTTACTACCT GGAGTAGGAGGGACATCT	*gfp*
gfp gerPE For	GGCATGGATGAACTATACAAATAAGGAGACT GAAAAATTATGTTGCATCA	*gfp*
gfp gerPE Rev	CCAGTGAAAAGTTCTTCTCCTTTACTTTGTGC GGAAGGTTCATCTGTAAT	*gfp*
gfp gerPF For	CATGGCATGGATGAACTATACAAATAATTCA TATAGTAATTACAAAGTTT	*gfp*
gfp gerPF Rev	GTGAAAAGTTCTTCTCCTTTACTCGCTGTTCC AATCTGATCTTGATCTG	*gfp*

pHT315 *gfp* Rev	GTTGTAAAACGACGGCCAGTGAATTCTTATTT GTATAGTTCATCCATGCC	*gfp*

613

614

615 Table 5 Oligonucleotide primers used to create *gfp*-fusions to defined spore coat proteins

Strain	Primer	Sequence (5' to 3')
BclA-gfp	pHT315 *bclA* For	GCTATGACCATGATTACGCCAAGCTTCTTCCA AATCAATCATATGTTATA
	bclA gfp Rev	CAGTGAAAAGTTCTTCTCCTTTACTAGCGATT TTTTCAATAATAATAGAT
	bclA gfp For	ATCTATTATTATTGAAAAAATCGCTAGTAAAG GAGAAGAACTTTTCACTG
	pHT315 *gfp* Rev	GTTGTAAAACGACGGCCAGTGAATTCTTATTT GTATAGTTCATCCATGCC
cotD-gfp	pHT315 *cotD* For	GCTATGACCATGATTACGCCAAGCTTTGCCAC CACCATCTCCGTATGC
	cotD gfp Rev	CCAGTGAAAAGTTCTTCTCCTTTACTCTTTTTA AATATTCCACCAACG
	cotD gfp For	CGTTGGTGGAATATTTAAAAAGAGTAAAGGA GAAGAACTTTTCACTGG
sleL-gfp	pHT315 *sleL* For	CTATGACCATGATTACGCCAAGCTTCATACCA CTCAGGATATAACTTTTT
	sleL gfp Rev	CAGTGAAAAGTTCTTCTCCTTTACTGCCCTTTT TCGTAATCGTAAAGTTT
	sleL gfp For	AAACTTTACGATTACGAAAAAGGGCAGTAAA GGAGAAGAACTTTTCACTG
cwlJ-gfp	pHT315 *cwlJ* For	GCTATGACCATGATTACGCCAAGCTTAGATAC CAAAGTAGGCTCAATTAC
	gfp cwlJ Down	CCAGTGAAAAGTTCTTCTCCTTTACTATATAC GCTAGGGCAGTCTTCGCC
	cwlJ gfp Up	GGCGAAGACTGCCCTAGCGTATATAGTAAAG GAGAAGAACTTTTCACTGG
	cwlJ gfp Down	TCCCTCCTCATTTTCATCTCTTATTTGTATAGT TCATCCATGCC
	gfp gerQ Up	GGCATGGATGAACTATACAAATAAGAGATGA AAATGAGGAGGGA
	pHT315 *gerQ* down	CGACGTTGTAAAACGACGGCCAGTGAATTCTT ATGGTCTTGGAGTATAAG

616

617

Figure legends

Figure 1 Schematic of a bacterial spore. The major cellular structures evident in thin section transmission electron microscopy images are shown. The spore coat can typically be sub-divided to outer and inner coat structures, with the pattern of striation depending on the species. The exosporium is present in some species, including *B. cereus*, but is absent in others, including *B. subtilis*.

Figure 2 Germination of *B. cereus gerP* spores in response to nutrient and non-nutrient germinants. Spores at an OD_{600} of 1 were suspended in buffer supplemented with defined germinants and the resultant changes in absorbance monitored as described in the Materials and Methods. Key to germinants: circles – 100 mM alanine (red, wild type; blue, *gerP*); triangles - 50 mM CaDPA (red, wild type; blue, *gerP*); squares – 1 mM dodecylamine (red, wild type; blue, *gerP*). The + sign represents wild type spores in buffer without germinant.

Figure 3 Fluorescence microscopy of *B. cereus* 14579 sporulating cells and spores with plasmid borne copies of (a) and (b) *gerPA-gfp*, (c) and (d) *gerPB-gfp*, (e) and (f) *gerPC-gfp*, (g) and (h) *gerPD-gfp*, (i) and (j) *gerPE-gfp*, and (k) and (l) *gerPF-gfp*. Expression of the various genes was controlled by native *gerP* operon regulatory sequences. Red fluorescence is associated with the lipophilic FM4-64 dye, which was used to visualise cell membranes. The scale bar represents 5 µM.

Figure 4 The locations of several GFP-fusion proteins with respect to the spore centre were estimated using the ELM image analysis technique. All of the GerP proteins were located near to the CLEs SleL and CwlJ, in the inner coat. The number of analysed spores and the residual error of the model fit are shown, and indicate that more accurate estimates were obtained within sporulating cells, just prior to mother cell lysis, than with mature spores which produced larger residuals attributed to clumping.

Figure 5 Phase contrast and fluorescence microscopy of sporulating *B. cereus gerPA* cells with plasmid borne copies of (a) and (b) *gerPA-gfp*, (c) and (d) *gerPB-gfp*, (e) and (f) *gerPC-gfp*, (g) and (h) *gerPD-gfp*, (i) and (j) *gerPE-gfp*, and (k) and (l) *gerPF-gfp*. None of the remaining GerP proteins can localise around the developing forespore in the absence of GerPA. The scale bar represents 5 µM.

Figure 6 Establishing the localisation hierarchy for GerP proteins. Phase contrast and fluorescence microscopy images of sporulating *B. cereus cotE* cells [(a) and (b)], and *safA* cells [(c) and (d)], both carrying plasmid borne *gerPA-gfp* under control of its native promoter. The GerPA-GFP protein is observed to localise around the developing forespore in the *cotE* background. The same protein is expressed in the *safA* strain but fails to localise, indicating that GerPA, and by extension all GerP proteins, are SafA dependent. These observations are consistent with an inner coat location for the GerP proteins. The scale bar represents 5 µM.

Figure 7 Fluorescence microscopy and super-resolved reconstructions of *B. subtilis* wild type spores [(a) and (b)], and *gerP* spores [(c) and (d)], stained with FITC-dextrans with an average molecular mass of 10 kDa. The super-resolved reconstructions are generated by feeding precise structure parameters from the fluorescence images back into the ellipsoid model for its image, while decreasing the inferred point spread function to remove instrumental blurring (9). The scale bar represents 5 µM.

Figure 8 The mid-point radial locations of regions of *B. subtilis* spores fluorescently-stained with FITC-dextran molecules were inferred using the ELM image analysis technique. The number of analysed spores and average residual error of the model fits are also shown for each case.

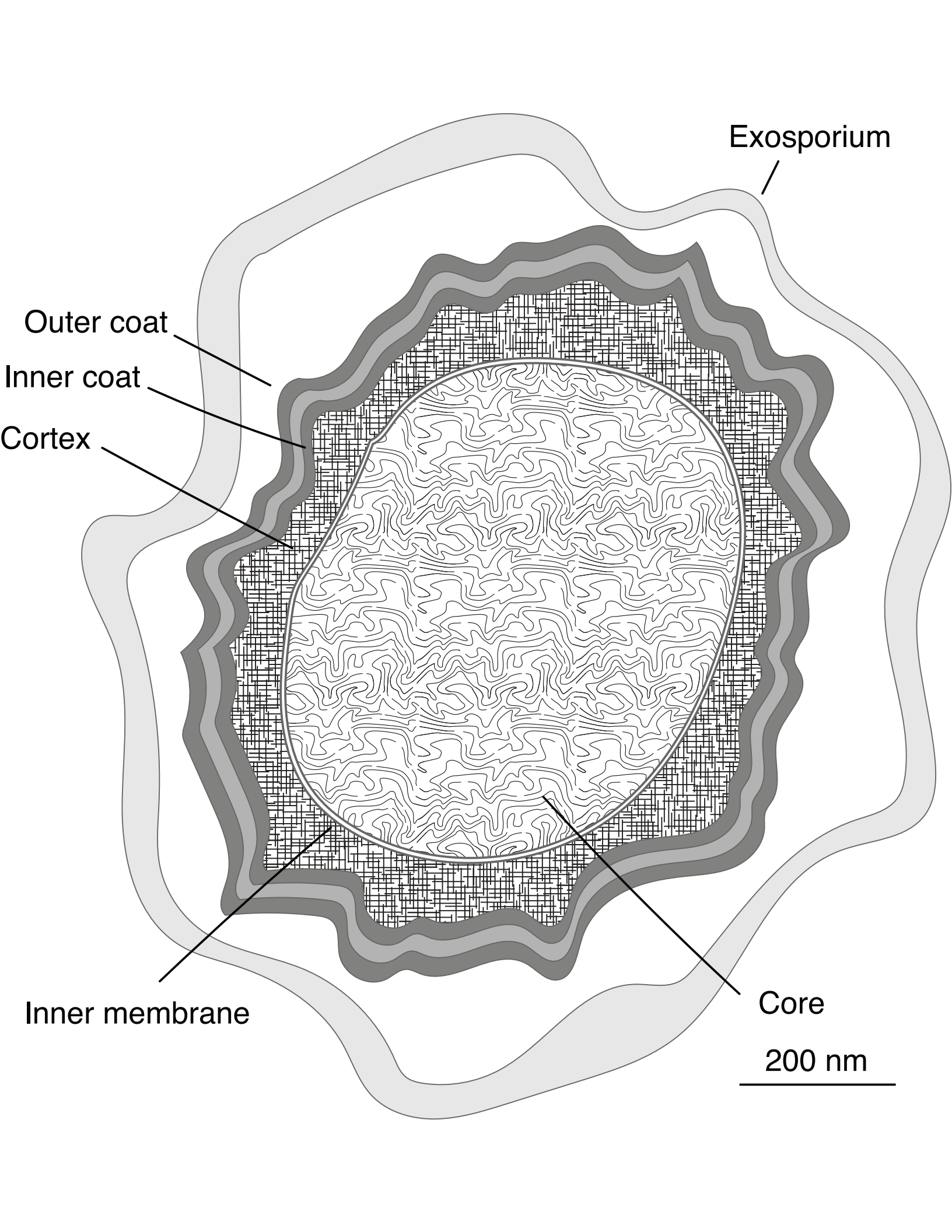
Exosporium
Outer coat
Inner coat
Cortex
Inner membrane
Core
200 nm

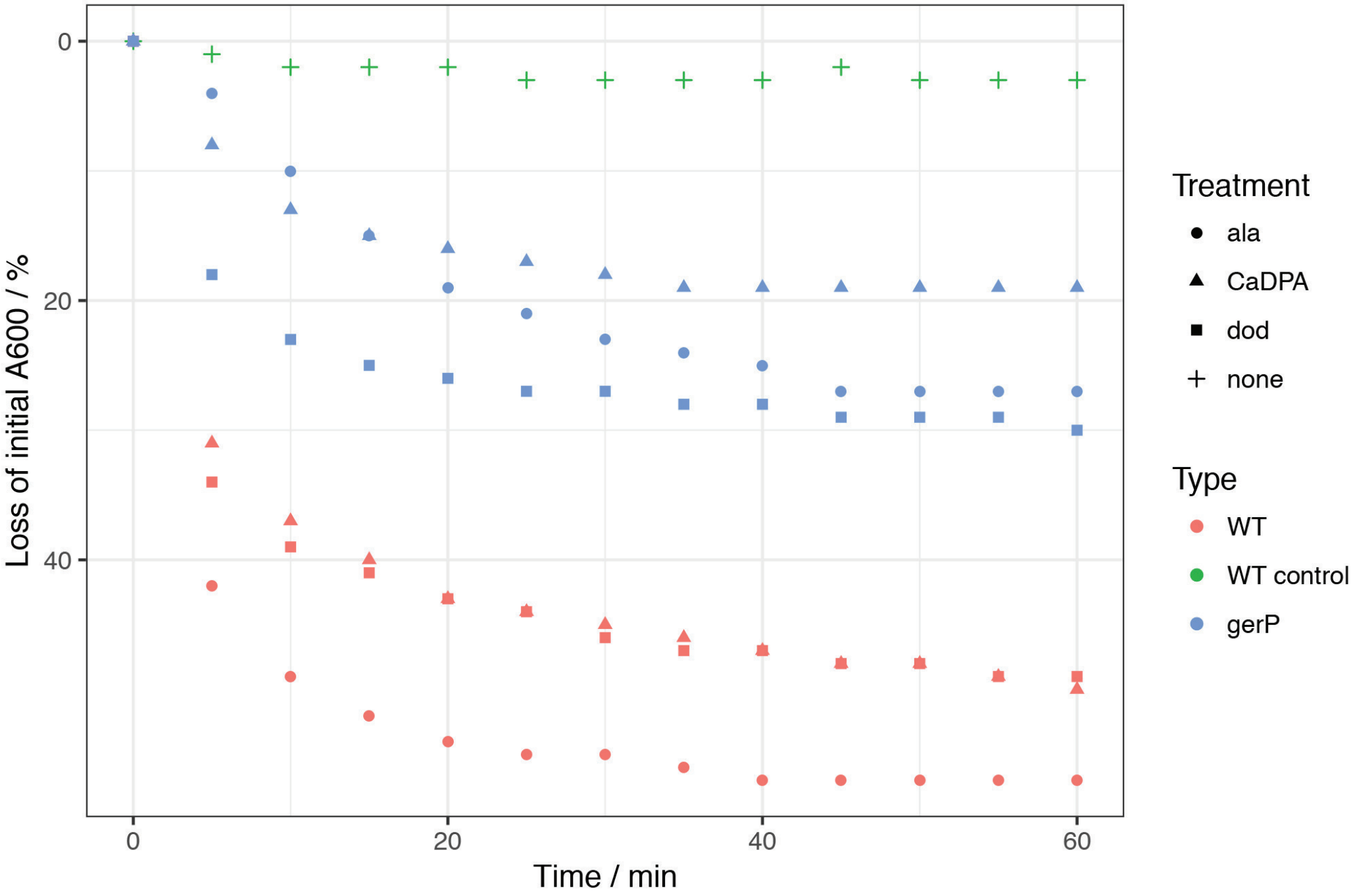
Loss of initial A600 / %
0
20
40
0
20
40
60
Time / min
Treatment
ala
CaDPA
dod
none
Type
WT
WT control
gerP

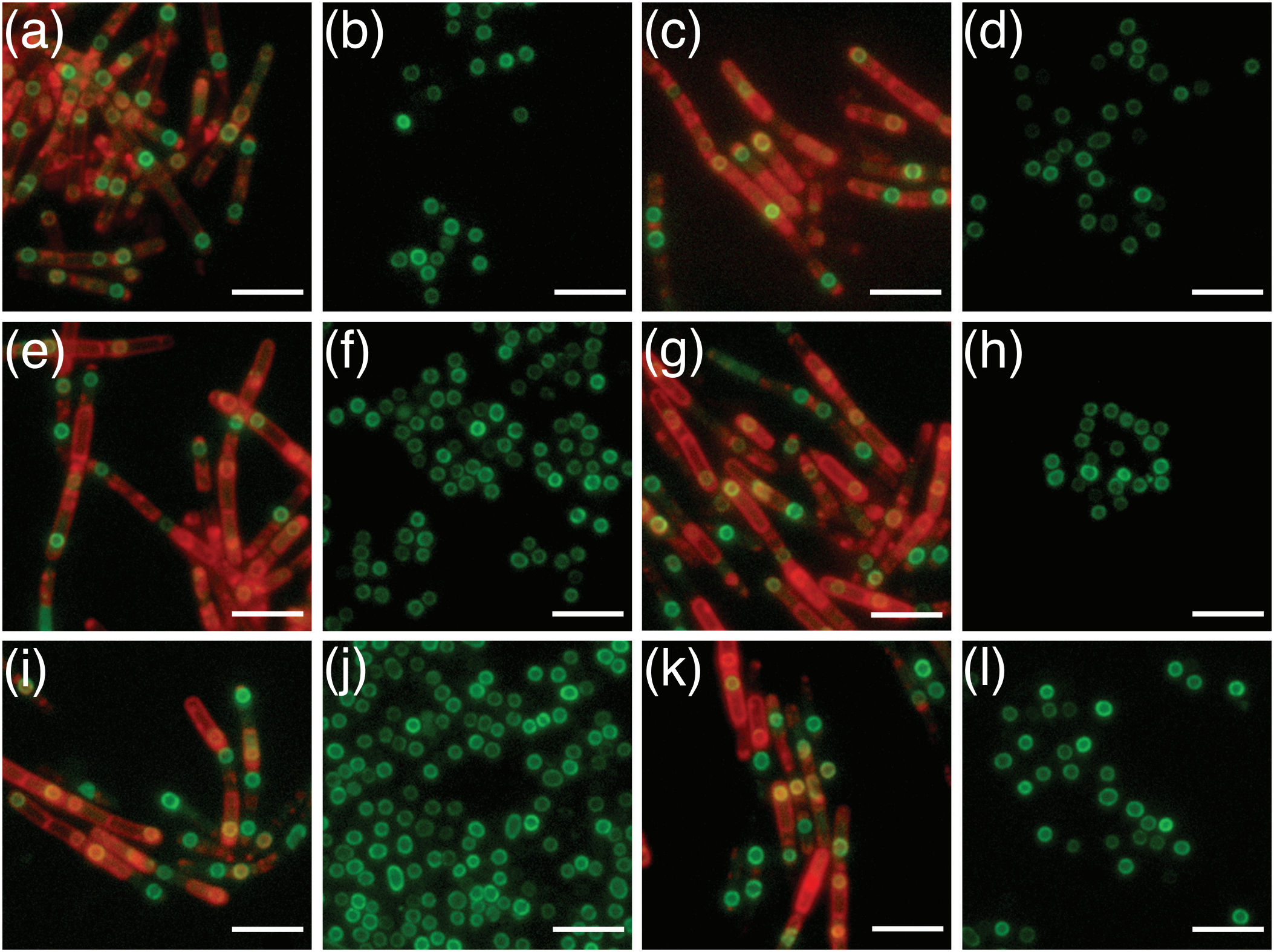
(a)
(b)
(c)
(d)
(e)
(f)
(g)
(h)
(i)
(j)
(k)
(l)

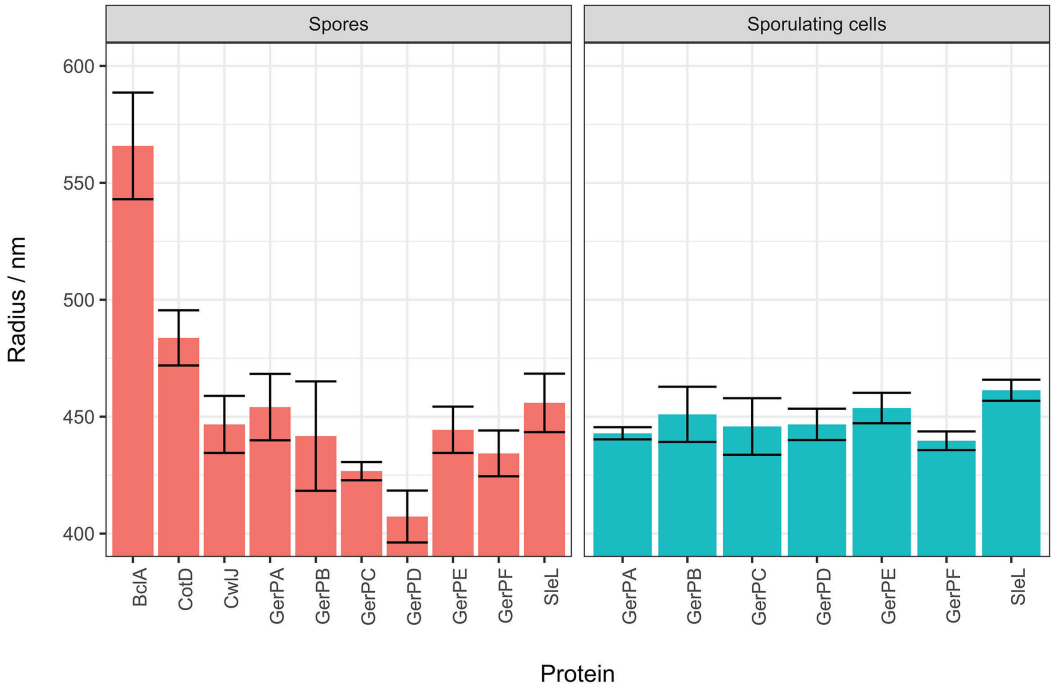
Spores
Sporulating cells
Radius / nm
600
550
500
450
400
BclA
CotD
CwlJ
GerPA
GerPB
GerPC
GerPD
GerPE
GerPF
SleL
Protein

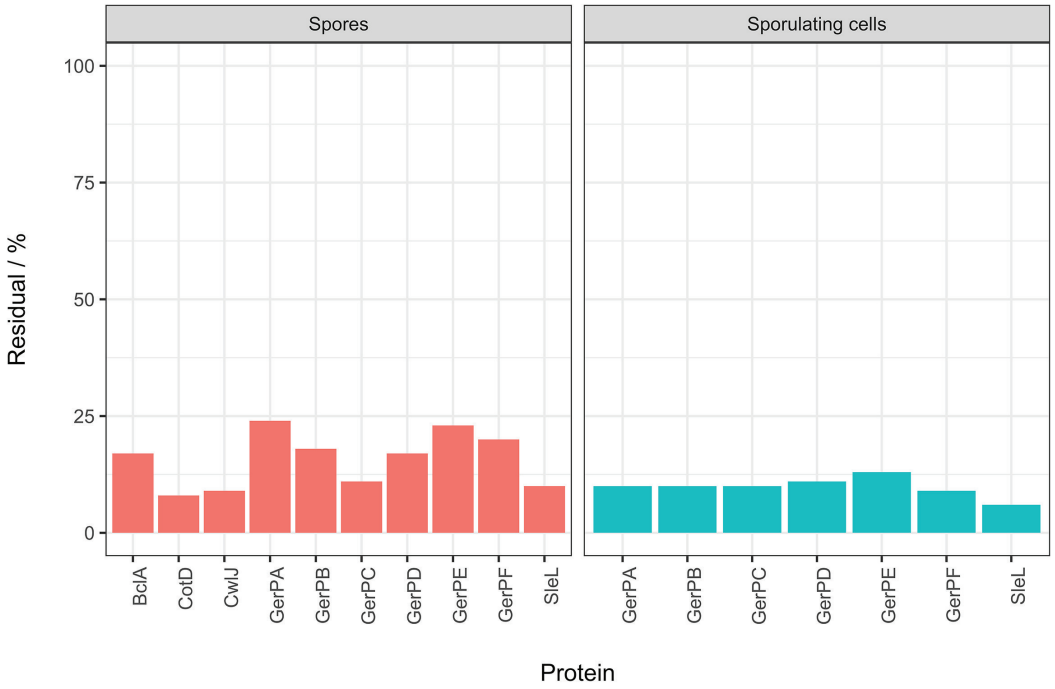
Spores
Sporulating cells
Residual / %
100
75
50
25
0
BclA
CotD
CwlJ
GerPA
GerPB
GerPC
GerPD
GerPE
GerPF
SleL
Protein

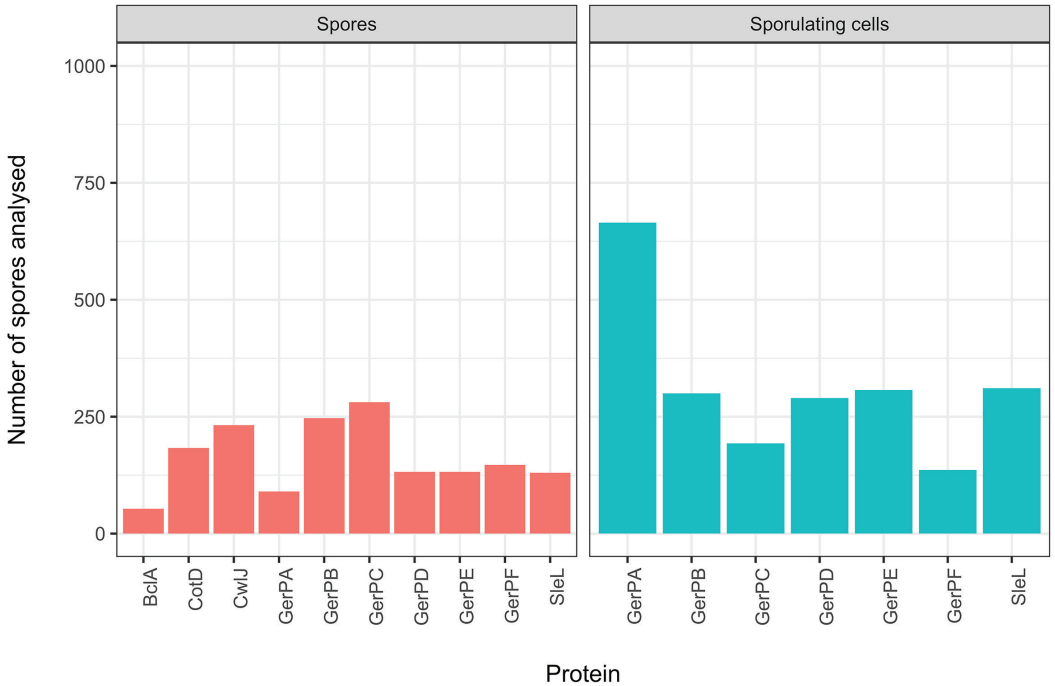
Spores
Sporulating cells
Number of spores analysed
1000
750
500
250
0
BclA
CotD
CwlJ
GerPA
GerPB
GerPC
GerPD
GerPE
GerPF
SleL
Protein

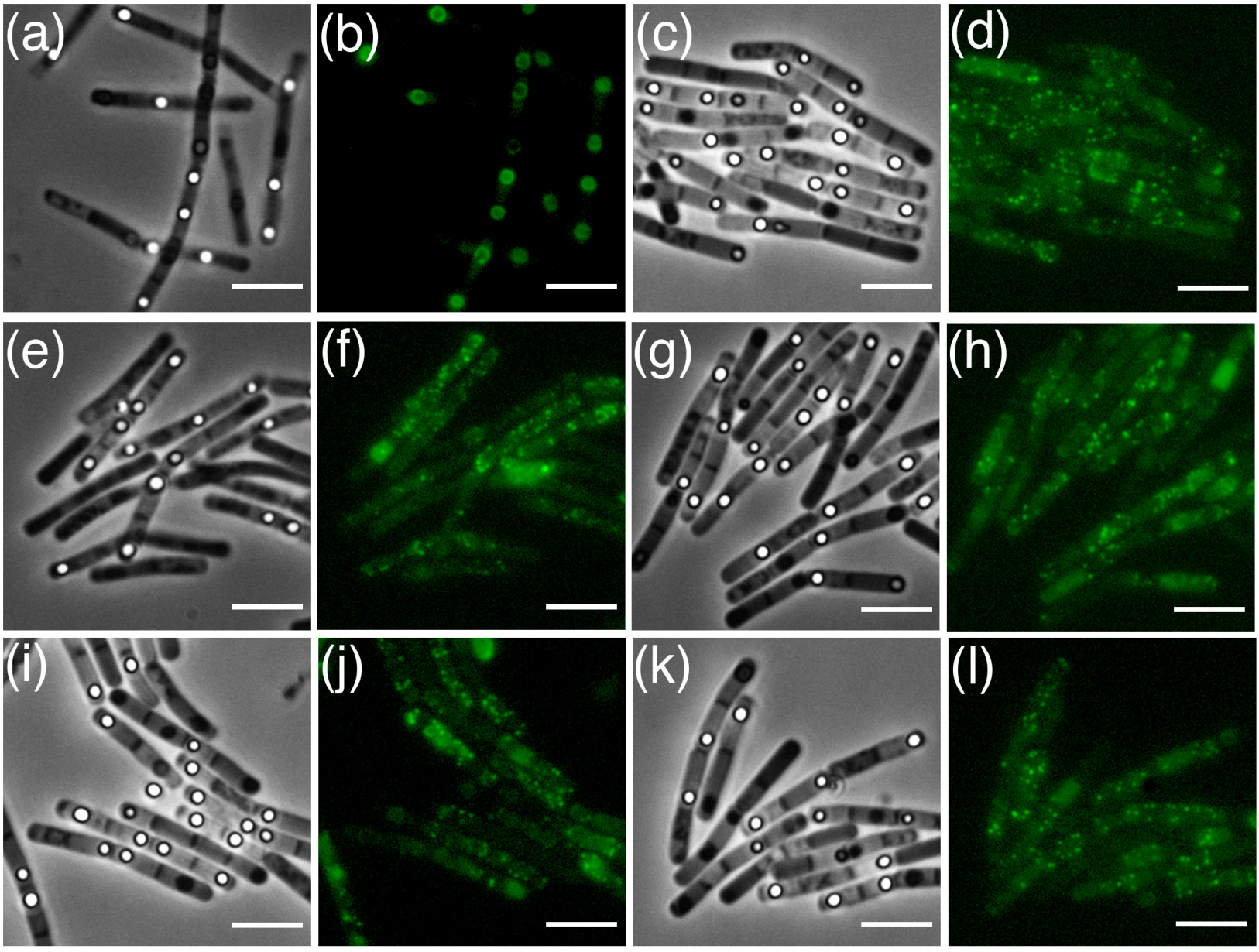
(a)
(b)
(c)
(d)
(e)
(f)
(g)
(h)
(i)
(j)
(k)
(l)

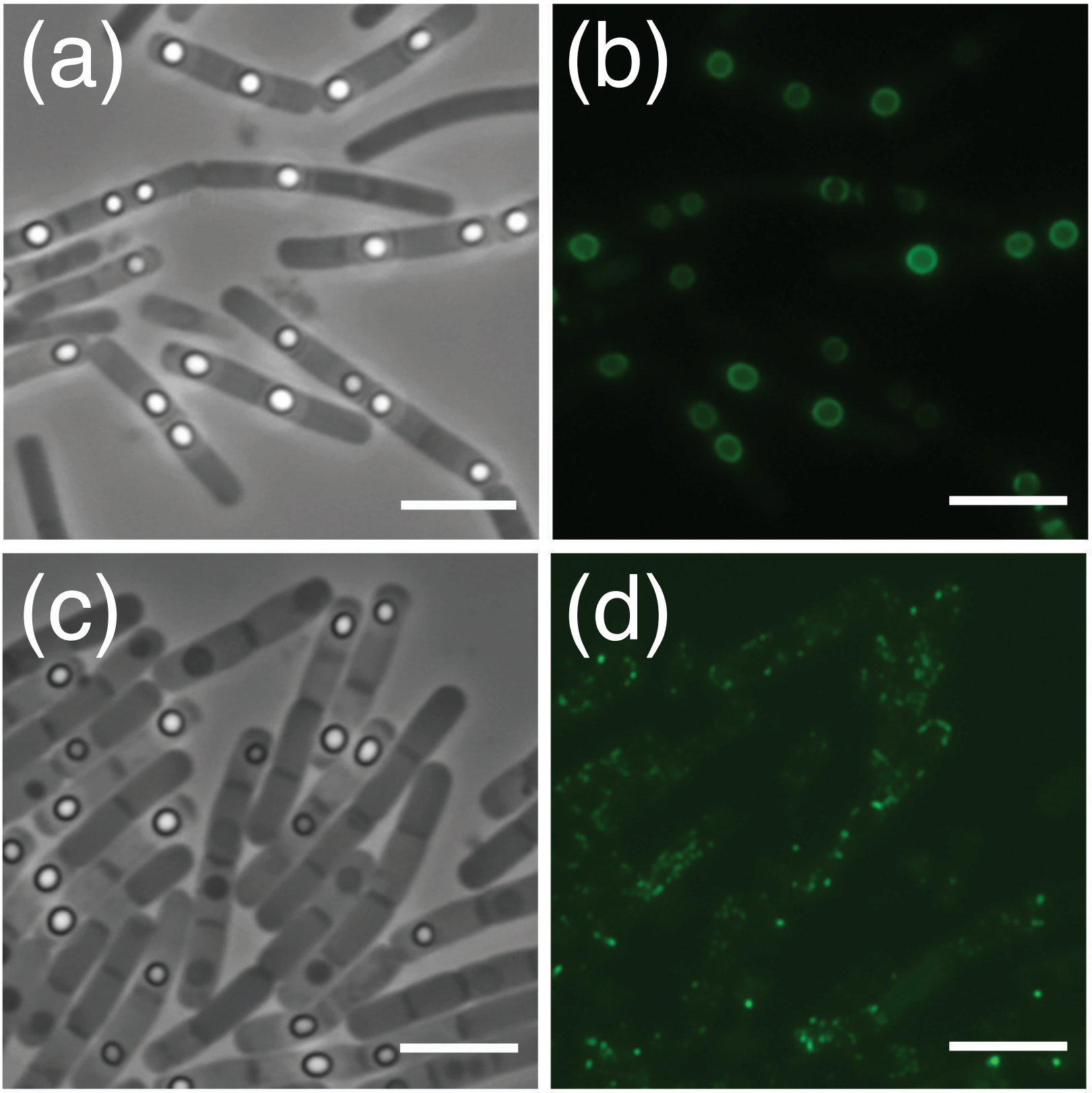
(a)
(b)
(c)
(d)

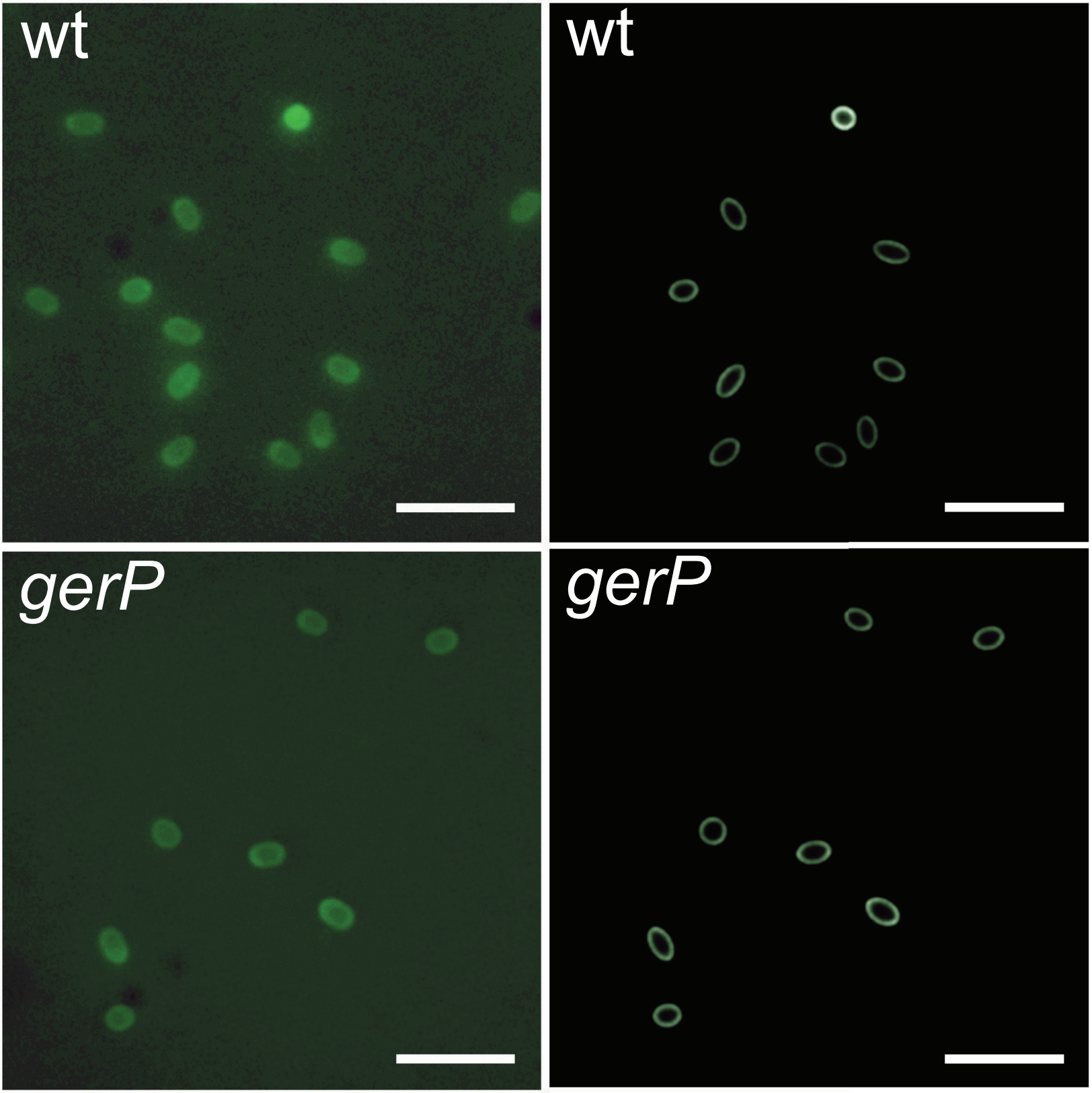
wt
wt
gerP
gerP

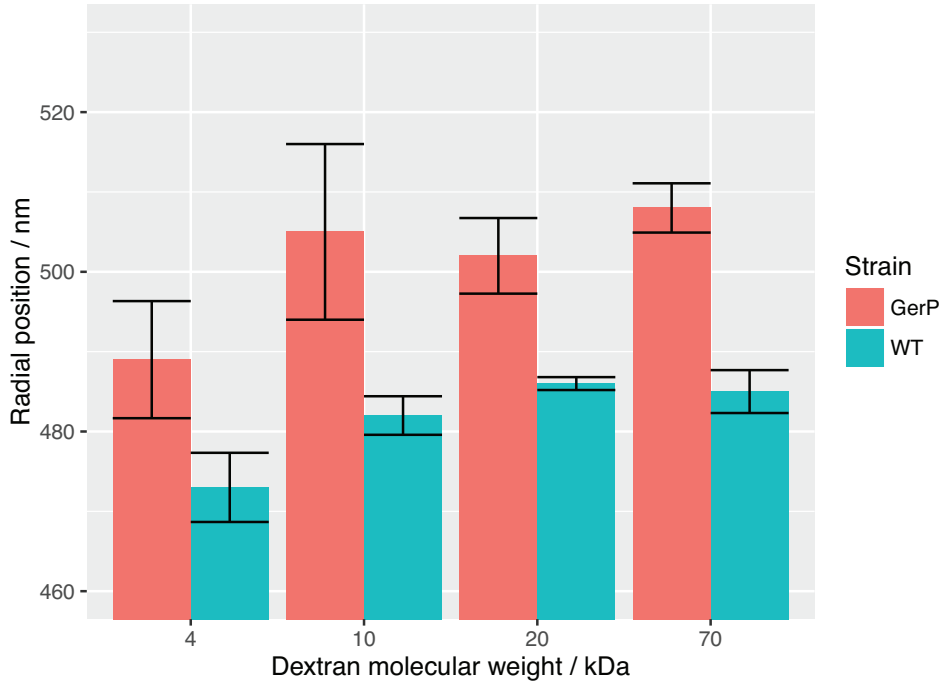
520
500
480
460
Radial position / nm
4
10
20
70
Dextran molecular weight / kDa
Strain
GerP
WT

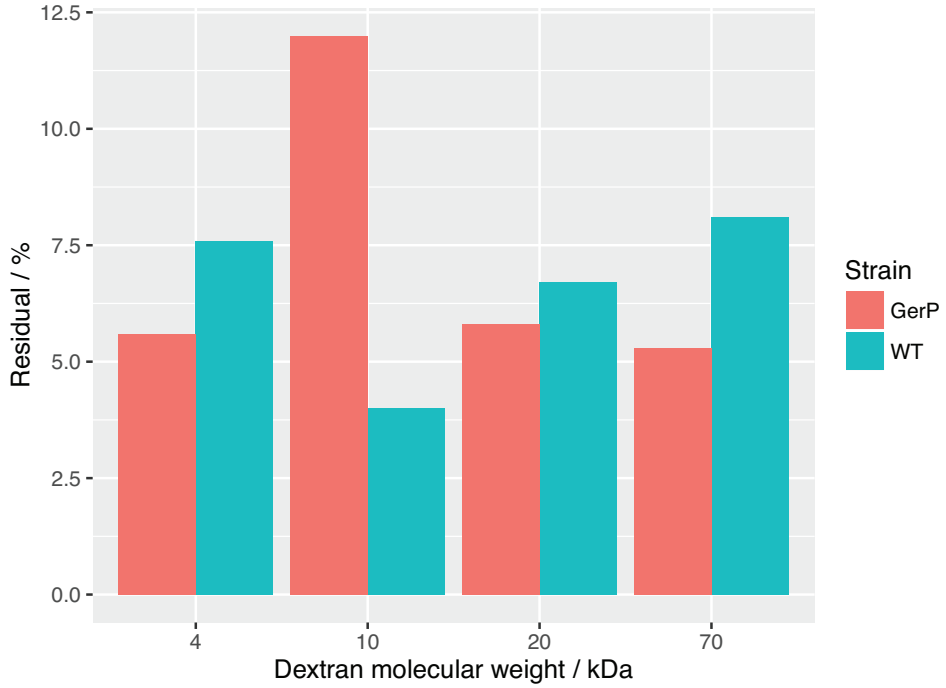
12.5
10.0
7.5
5.0
2.5
0.0
Residual / %
4
10
20
70
Dextran molecular weight / kDa
Strain
GerP
WT

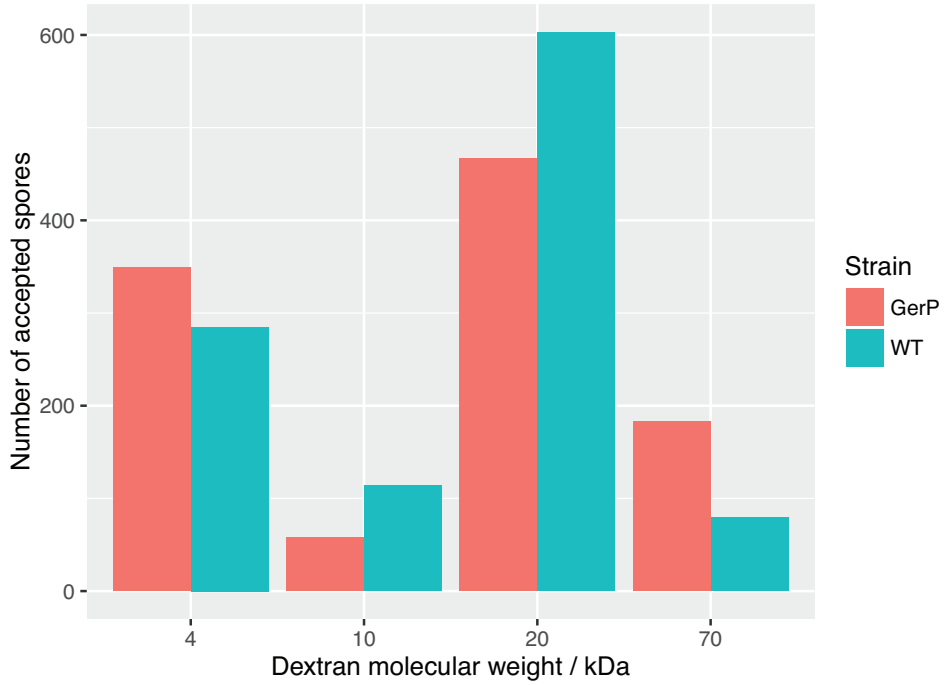
600
400
200
0
Number of accepted spores
4
10
20
70
Dextran molecular weight / kDa
Strain
GerP
WT